

A macrocyclic approach to transition metal and uranyl Pacman complexes

Jason B. Love

Received (in Cambridge, UK) 2nd March 2009, Accepted 18th March 2009

First published as an Advance Article on the web 27th April 2009

DOI: 10.1039/b904189c

Multielectron redox chemistry involving small molecules such as O₂, H₂O, N₂, CO₂, and CH₄ is intrinsic to the chemical challenges surrounding sustainable, low-carbon energy generation and exploitation. Compounds with more than one metal reaction site facilitate this chemistry by providing both unique binding environments and combined redox equivalents. However, controlling the aggregation of metal cations is problematic, as both the primary coordination spheres of the metals and the metal–metal separations have to be defined carefully. We described recently a series of pyrrole-based macrocyclic ligands designed to manage metal aggregation and form molecular multimetallic complexes. In particular, we have shown that these compartmentalised Schiff-base calixpyrroles generally form rigid Pacman complexes that prescribe well-defined, metallo microenvironments within the molecular cleft. This article will review the development of this chemistry and its context, and will highlight structural facets and reaction chemistry of metal complexes from across the periodic table.

Introduction

Compounds that promote efficient chemical transformations of small molecules, such as O₂, H₂O, alkanes, CO₂, and N₂, are fundamental to the development of technologies for sustainable, low-carbon energy generation and exploitation. For example, the catalytic oxidation of water to evolve oxygen¹ and its microscopic reverse reaction, the reduction of oxygen to water,² are key multielectron redox reactions that must occur in the conversion of solar to chemical energy using solar

fuel cells and in the use of this stored chemical energy in hydrogen fuel cells.³

Strategies towards the development of suitable catalysts for these multielectron redox processes have often taken inspiration from nature which takes advantage of metalloenzymes that contain bi- or multimetallic reaction sites that are organised precisely.^{4,5} As such, the design of ligands that can promote the construction of bi- and multimetallic complexes that imitate or surpass enzymes as catalysts in multielectron redox processes has both a long held fascination and strategic significance.⁶

This approach is exemplified by the synthesis and chemistry of cofacial or Pacman diporphyrin complexes, in which the well-known coordinative properties of the porphyrin are combined with exceptional control of the intrametallic separation by a rigid and well-defined spacer between the two porphyrinic compartments (Fig. 1).^{7–9} The resulting bimetallic molecular cleft facilitates extensive stoichiometric and catalytic small

EaStCHEM School of Chemistry, University of Edinburgh, Joseph Black Building, The King's Buildings, West Mains Road, Edinburgh, UK EH9 3JJ. E-mail: jason.love@ed.ac.uk; Fax: +44 (0)131 6504743



Jason Love

Jason Love obtained his PhD in 1993 from Salford University with Prof. John Spencer. He undertook postdoctoral positions with Prof. Geoff Cloke (Sussex), Prof. Michael Fryzuk (UBC, Vancouver), and Prof. Martin Schröder (Nottingham) before taking a lectureship and Royal Society URF (1999–2004) at Sussex in 1999. In 2001, he moved to Nottingham University and then to his current post at Edinburgh University in 2007 as a Senior Lecturer. His

research interests focus on small molecule chemistry and the use of ligand design strategies to form well-defined complexes of metals from across the periodic table.

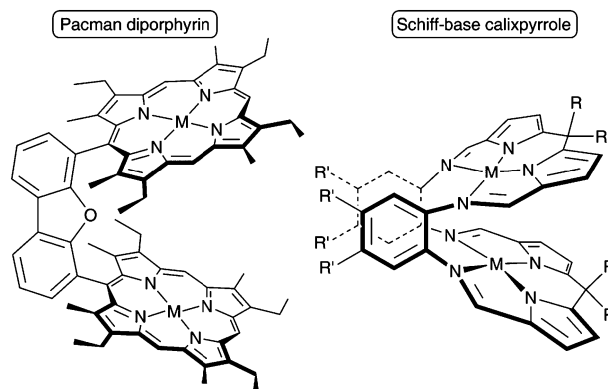


Fig. 1 Pictorial comparison of binuclear complexes of Pacman diporphyrins and Schiff-base calixpyrroles.

molecule chemistry, such as oxygen redox and atom-transfer reactions,^{7,8,10} hydrogen activation,¹¹ nitrogen reduction,¹² and even alkane activation.¹³

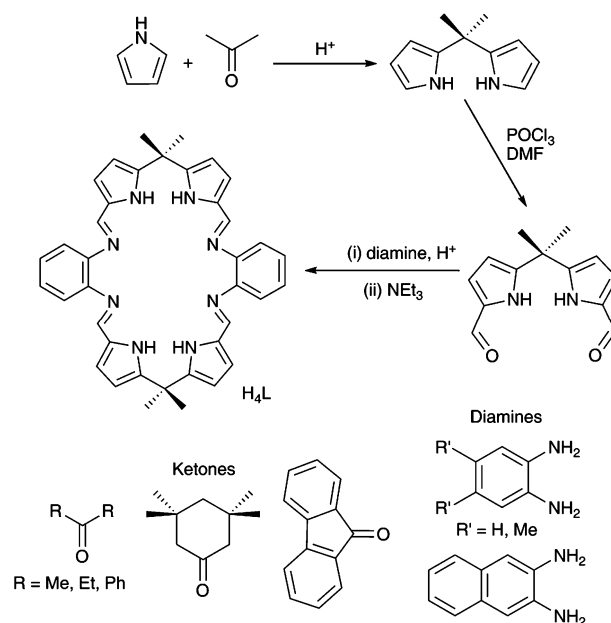
Schiff-base polypyrrolic macrocycles that combine the coordinative and physicochemical properties of the pyrrole group with the exceptional design characteristics and synthetic versatility of macrocyclic Schiff-base condensation procedures can be seen as alternatives to these porphyrinic ligands, which are often arduous to synthesise and isolate.^{14,15} These former features are particularly apposite to the synthesis of ligands that can direct bi- and multinuclear transition metal complex formation. Furthermore, polypyrrolic macrocycles can exhibit a rich and diverse chemistry. The flexible frameworks of calixpyrroles can accommodate a variety of transition metals and f-block elements in a range of oxidation states, from which elegant transformations of the macrocycle itself or the activation of small molecules can ensue.¹⁶ Calixpyrroles and their derivatives are also extremely efficient and sometimes selective anion-binding agents.¹⁷ Schiff-base polypyrrolic lanthanide complexes such as motexafin lutetium are receiving considerable attention as photodynamic therapy agents,¹⁸ and similar iminopolypyrroles can complex actinide cations such as uranyl and late first-row transition metals.¹⁹

We describe here an overview of our work in this area, in particular the development of a new class of Schiff-base polypyrrolic macrocycle and its features that promote the formation of bi- and multinuclear complexes (Fig. 1) that are reminiscent of cofacial or Pacman diporphyrins.

Macrocyclic synthesis and structures

Using a method developed by Sessler and co-workers for the synthesis of Schiff-base expanded porphyrins, we found that methanolic solutions of *meso*-disubstituted diformyldipyrromethanes react with 1,2-aromatic diamines in the presence of TsOH to generate cleanly the orange and crystalline [2 + 2] macrocyclic products $H_4L(TsOH)_4$ in high yield (Scheme 1).^{20,21}

No reaction takes place without the acid template,²² and, as described independently by Sessler and co-workers, a variety of acids can mediate this [2 + 2] cyclisation reaction.²³ Treatment of these acid salts with a base such as NaOH or triethylamine in alcoholic solvents precipitates quantitatively the acid-free macrocycles H_4L that can be isolated simply by suction filtration. Significantly, the overall synthetic procedure to form H_4L is efficient, modular, uses inexpensive starting materials (pyrrole/ketone/diamine) and can be carried out to yield >30 g. This contrasts to the synthesis of cofacial diporphyrins which are often low yielding, multiple step procedures that require the extensive use of column chromatography. These yellow, air-stable, amorphous materials are poorly soluble in common organic solvents but, with the addition of protic solvents such as water or ethanol, crystalline materials were isolated and characterised by X-ray crystallography (Fig. 2). The Schiff-base calixpyrrole has been found to adopt two different structural motifs in the presence of a protic solvent: a non-planar, bowl-like conformation around two hydrogen-bonded molecules of ethanol (Fig. 2, left) and a Pacman-type conformation centred on a molecule of water



Scheme 1 The synthesis of the Schiff-base calixpyrroles used by us in this research (*n.b.* for simplicity, L is used generically for this series of ligands and their complexes).

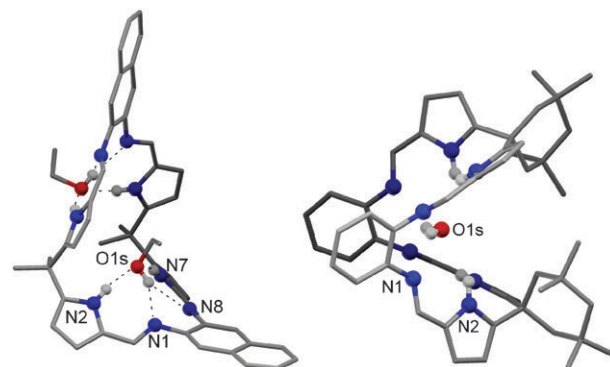


Fig. 2 Ball and stick representations of the X-ray crystal structures of the solvated macrocycles $H_4L \cdot (EtOH)_2$ and $H_4L \cdot (H_2O)$ (*n.b.* left: L derived from diaminonaphthalene; right: from tetramethylcyclohexanone).

(Fig. 2, right). Both of these structures illustrate the capacity of these macrocycles to act both as hydrogen-bond donors, through interactions between pyrrole NH protons and O-acceptor, and as hydrogen-bond acceptors, through interactions between the imine N atoms and the ethanolic OH proton. Furthermore, similar structural motifs were identified at low temperature in solution by NMR spectroscopy. These hydrogen-bonding interactions are commensurate with the development of Schiff-base calixpyrroles and acyclic iminopyrrole compounds as effective anion-binding agents.²⁴ The non-planar structures adopted are unlike those seen for related expanded porphyrins and Schiff-base porphyrin analogues,²⁵ and are a consequence of both the conformational flexibility and the lack of extended π -conjugation that results from the incorporation of sp^3 -hybridised, *meso*- CMe_2 groups into the macrocyclic framework. It is clear from the solid state structures that either the *meso*- CMe_2 groups or the aryl groups can

act as hinges that compartmentalise different two N_4 -donor sets; as such, two different metal binding modes would be expected.

Binuclear Pacman complexes

Pd complexes

The reactions between $Pd(OAc)_2$ and H_4L in the presence of base result in the sole formation of red, binuclear palladium complexes $[Pd_2(L)]$ in good yields.^{20,21} The X-ray crystal structures of this series of complexes were determined, and a representative example is shown in Fig. 3. Each palladium cation adopts a square-planar geometry with limited out-of-plane displacement and two distinct sets of Pd–N bond distances are observed, the shorter between the palladiums and the pyrrolic nitrogen atoms and the longer between the palladiums and the four imine nitrogen atoms. The presence of the sp^3 -hybridised *meso*-CMe₂ link between the planar imine-pyrrole chelates allows a degree of flexibility within each PdN_4 compartment, causing the chelates to curve away from each other. Importantly, the metal–ligand geometry, coupled with the presence of the rigid 1,2-disubstituted aryl spacers between the two PdN_4 -donor compartments, results in a bimetallic molecular cleft structure in which the *o*-aryl units are offset face-to-face π -stacked and act as hinges that promote a wedged arrangement of the two PdN_4 square planes. This gross structural motif is similar to those observed for single-pillared or ‘Pacman’ diporphyrin complexes, in which the spatial separation between two metal porphyrins is rigidly defined by an appropriate, generally aromatic, spacer unit.

These structures are best compared by defining three variables: the metal–metal separation ($M \cdots M$), and ‘bite’ and torsional twist angles between the two MN_4 compartments. The Pd \cdots Pd separation varies between 3.544 and 4.120 Å, and, in contrast to Pacman diporphyrinic analogues in which the $M \cdots M$ separation can vary between 3.5 and 7.8 Å (this range is dependant on the nature of the spacer in the Pacman ligand),²⁶ represents a small and rigidly-constrained vertical translation. Furthermore, the X-ray crystal structures of the dipalladium Pacman bis(porphyrin) complexes $[Pd_2(DPX)]$ and $[Pd_2(DPD)]$, where DPX and DPD are dibenzoxanthene and dibenzofuran pillars, respectively,

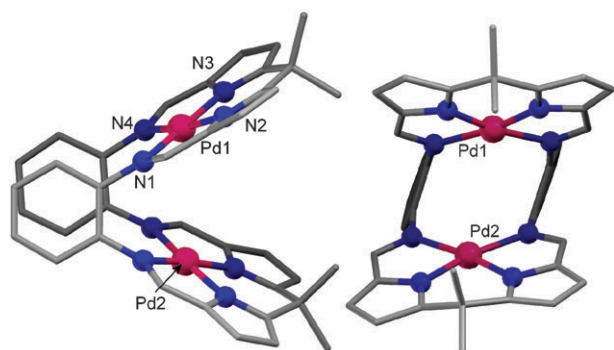


Fig. 3 Side and face-on views of the structure of the binuclear Pacman complex $[Pd_2(L)]$.

show cofacial arrangements of the porphyrins with considerably different Pd \cdots Pd separations [3.97 Å (DPX) and 6.81 Å (DPD)].²⁷ Dicobalt Pacman diporphyrins in which the two porphyrins are linked by an *o*-phenylene spacer display intrametallic separations >6.0 Å,²⁸ while dizinc analogues are truly cofacial, and show short, interplanar separations (~ 3.4 Å) due to favourable π -stacking interactions.²⁹ The intrametallic separation in $[Pd_2(L)]$ complexes appears to be intrinsically-linked to both the bite (range 53–62°) and twist (range 11–29°) angles, which are dependant on ligand substitution patterns. Increased offset face-to-face π -stacking overlap of the hinge aryl groups causes an increased twist angle and decreased bite angle, which results in shorter Pd \cdots Pd distances. The effect of substitution of the *meso*-CMe₂ groups with CPh₂ is less clear, although this does result in an increased twist angle as a consequence of the more sterically-demanding *endo*-phenyl substituents. It therefore appears that these new Pacman molecules ‘chew’ rather than ‘bite’.

The syntheses of related di-iron complexes of L, $[Fe_2(\mu-O)(L)]$, were carried out by Sessler and co-workers, who found that similar Pacman structural motifs were adopted in the solid state.³⁰ In these compounds, the binuclear molecular cleft structure is reinforced by the metal-bridging oxo-group which allows for no torsional twist (0.3°) and promotes a close $M \cdots M$ separation (3.145 Å). The significance of the *o*-aryl hinge in promoting the rigid Pacman structural motif is evident by comparison to similar binuclear ‘accordion’ Schiff-base diporphyrin and calixpyrrole complexes that have been characterised structurally by Bowman-James *et al.* (Fig. 4, left),³¹ and Brooker *et al.* (Fig. 4, right),³² respectively. In both of these cases, the presence of conformationally-labile alkyl chain linkers between the two N_4 -donor compartments results in flattened structures in which the metals are highly separated (5.39 to 8.38 Å).

Cu complexes

Both we²¹ and Sessler and co-workers³³ have synthesised a series of binuclear copper(II) complexes $[Cu_2(L)]$ and have shown that constrained Pacman structures are adopted, both in the solid state by X-ray crystallography and in solution by EPR spectroscopy. Crystallisation of one of these compounds in the presence of pyridine resulted in the mono-pyridine adduct $[Cu_2(py)(L)]$ which exemplifies the constrained nature

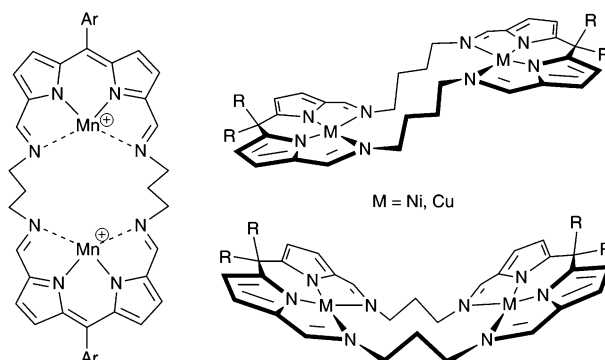


Fig. 4 Binucleating Schiff-base calixpyrroles with N_4 -donor compartments linked by alkyl chains.

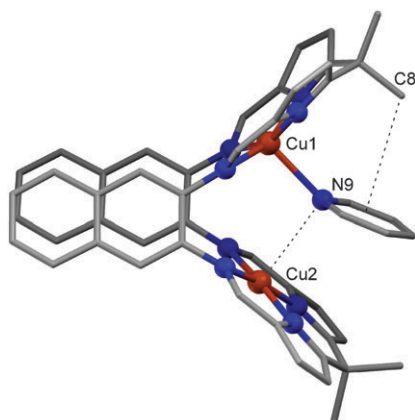


Fig. 5 Structure of $[\text{Cu}_2(\text{endo-py})(\text{L})]$ highlighting the in-cleft binding of pyridine and stabilising interactions (*n.b.* L derived from diamino-naphthalene).

of this class of macrocyclic complex. In the solid state (Fig. 5), it was found that the pyridine is bound unusually within the cleft in a *pseudo*-bridging manner. In this case, the two copper centres are different, with square pyramidal and square-planar geometries, and the molecule of pyridine has adopted a canted geometry in which the Cu1–N9 bond does not lie in the $\text{C}_5\text{H}_5\text{N}$ plane and results in a Cu1–N9-(pyridine-centroid) angle of 155° . This coordination geometry also maximises two further interactions: a face-to-face π -stacking interaction between pyridine and the Cu_2N_4 plane, and a hydrogen-bonding interaction between the C8 *meso*-methyl proton and the pyridine ring. Furthermore, to accommodate the pyridine, the macrocycle has expanded in bite angle and has undergone a 12° reduction in torsional twist which results in an increase of the Cu1...Cu2 separation to 4.014 Å. There are few solid state structures in which a pyridyl donor is bound between two Cu centres, and none in which this group is not a part of an extended ligand structure, for example, in terpyridine or (bis-imino)pyridine ligands.³⁴ In these latter examples, the pyridine bridges are asymmetric and are twisted with respect to the Cu...Cu vector due to the overall helicity of these dicopper systems.

With their increased lateral flexibility, bimetallic cofacial diporphyrins have been found to act as hosts for larger guest molecules, and in particular for guests incorporating two donor atoms that encourage bimetallic binding. For example, the dizinc complex $[\text{Zn}_2(\text{DPD})]$ acts as a 1 : 1 host for 2-aminopyrimidine, which is bound to both Zn ions within the diporphyrinic cavity.³⁵ Molecules such as DABCO and even C_{60} have been bound within Pacman clefts by using strategies that elongate the spacer between the two porphyrin units. For example, calixarene or diarylurea spacers provide a rigid, yet sufficiently elongated, separation between Zn(porphyrin units) to accommodate DABCO,³⁶ while the use of a *trans*-substituted $\text{PdCl}_2(\text{pyridylporphyrin})_2$ complex as a spacer results in a cavity large enough to host C_{60} .³⁷

Alternative binding modes for metal cations

It is evident that the complexation of two metal cations by the Schiff-base calixpyrrole L can result in the formation of

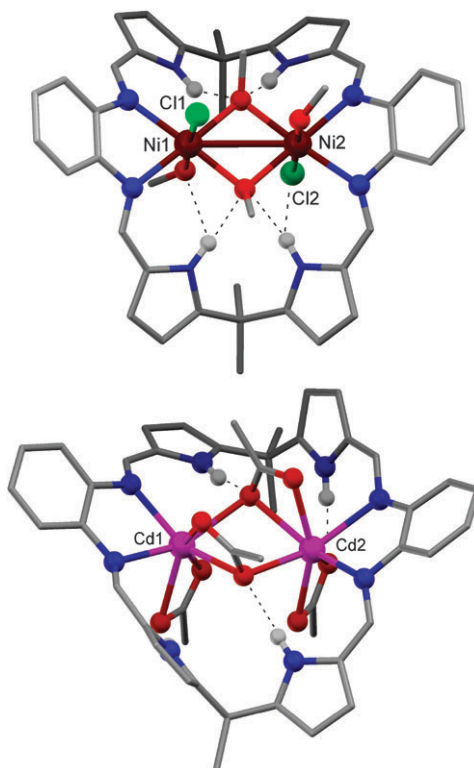


Fig. 6 Bowl-shaped, bridged binuclear complexes of H_4L .

Pacman-shaped complexes. However, unlike cofacial diporphyrins, the relative flexibility of the macrocycle that results from the incorporation of the *meso*- sp^3 -hybridised links allows for a variety of other metal binding modes. In particular, these alternatives make use of the propensity of the pyrrole hydrogens to partake in hydrogen-bonding, a feature that may have important consequences in the structure, bonding, and reactivity of the coordinated metals and their attendant ligands.³⁸ Indeed, we found that the reactions between hydrated NiCl_2 and H_4L in the presence of NET_3 did not result in the expected binuclear Pacman complexes, $[\text{Ni}_2(\text{L})]$, but instead formed hydroxy- or methoxy-bridged adducts $[\text{Ni}_2(\mu\text{-OR})_2\text{Cl}_2(\text{HOMe})_n(\text{H}_4\text{L})]$ ($\text{R} = \text{H}$, $n = 1$; $\text{R} = \text{Me}$, $n = 2$). Importantly, to access the Pacman complex, it was found necessary to first deprotonate the macrocycle under anaerobic conditions prior to reaction with anhydrous NiCl_2 .²¹

The structure of $[\text{Ni}_2(\mu\text{-OMe})_2\text{Cl}_2(\text{HOMe})_2(\text{H}_4\text{L})]$ (Fig. 6) revealed that the Ni^{II} centres are octahedral and bound solely to the imine nitrogen donors; the other equatorial sites are occupied by two methoxy bridges that link the metal centres and the axial positions of both cations are occupied by a chloride anion and a neutral methanol molecule in a transoid configuration. It is presumed that the methoxy groups derive from the deprotonation of methanol solvent under the basic reaction conditions. The pyrrole nitrogens remain protonated and are found to hydrogen-bond primarily to the methoxy-bridging ligands although close contacts between the pyrrole nitrogens and axial chloride and methanol ligands are also observed. The presence of the methoxy bridges results in a relatively short Ni...Ni separation of 3.122 Å, and is

comparable to those found in related binuclear Ni^{II} Schiff-base complexes.

A similar bowl-shaped macrocycle conformation was seen in the solid state structure of the binuclear cadmium complex [Cd₂(OAc)₄(H₄L)] in which the Cd cations bind solely to the imine nitrogens with the pyrrolic nitrogens remaining protonated (Fig. 6).³⁹ The Cd acetate environment comprises asymmetric terminal- and bridging-bidentate acetate coordination, a mode normally common in lanthanide complexes. Close interactions between the pyrrolic nitrogen and acetate oxygen atoms are evident and are consistent with intramolecular hydrogen-bonding. Furthermore, this structure is retained in solution, as ¹H NMR spectroscopy showed Cd-coupling to the imine H (*J*_{CdH} 30.3 Hz) consistent with complexation of the Cd^{II} cations to the imine nitrogens, and the presence of hydrogen-bonded pyrrolic NH resonances at 12.2 ppm.

Sessler and co-workers have also found that a variety of alternative bonding modes are accessible (Fig. 7). While the protonolysis reaction of H₄L with Fe₂(mesityl)₄ forms, after aerobic oxidation, the Fe^{III} Pacman complex [Fe₂(O)(L)], a similar reaction with the salt H₄L·(HCl)₂ generated [(FeCl)₂(μ-O)(H₂L)] in which the Fe^{III} cations are five-coordinate and bound to two imine nitrogens and one pyrrole.³⁰

The organometallic Ru complexes [(η⁶-C₆H₆)RuCl]₂(H₄L)]²⁺ and [(Cp*₂Ru(O₂))₂(H₄L)]²⁺ were also synthesised in which the pyrrole nitrogens remain protonated and hydrogen-bond to the ancillary Cl and O₂ ligands.⁴⁰ In these cases, the Ru cations bind to the macrocycle through the imine nitrogen donors and are disposed in an *anti*-conformation, in some part similar to the *anti*-conformation of the EtOH molecules in H₄L(EtOH)₂. Furthermore, the reactions between H₄L and Zn and Cd tetrafluoroborates resulted in the bowl-shaped binuclear complexes [M₂(μ-F₂)(μ-S)(H₄L)] (M = Zn, S = Me₂CO; M = Cd, S = H₂O).⁴¹ As with the above examples, the metal cations complex to the imine nitrogen donors, and the pyrrole protons are involved in hydrogen-bonding interactions with the ancillary bridging ligands.

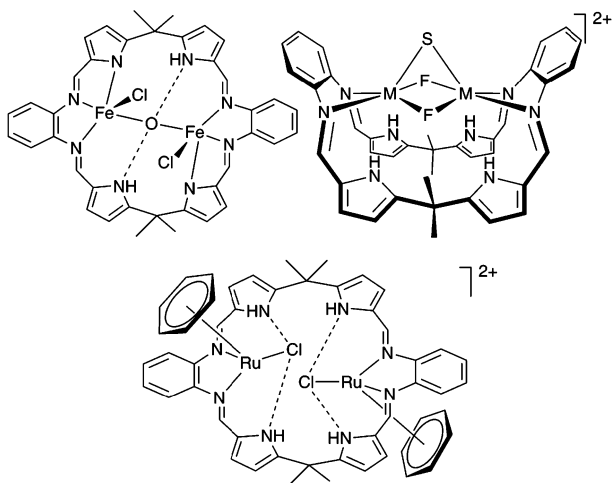


Fig. 7 Alternative coordination modes in binuclear complexes of H₄L (M = Zn, S = Me₂CO; M = Cd, S = H₂O).

Macrocycle expansion

While the generation of large macrocyclic structures can be favoured using Schiff-base condensation methods, the potential hydrolytic instability of the N=C imine bond(s) can result in undesirable ring opening, although this feature can be exploited in combinatorial Schiff-base self-assembly reactions.⁴² While exploring the formation of zinc complexes of L which should exhibit a rich reaction chemistry, we found that the reaction between H₄L and Zn(OAc)₂·2H₂O in boiling CHCl₃ formed the new Zn^{II} complex, [Zn(OAc)₂]₃(H₆L¹), in moderate, but consistent, yield.³⁹ The formulation of the new, metal-free, Schiff-base pyrrolic macrocycle H₆L¹ was inferred from ES-MS data and the structure of this macrocyclic product was described unambiguously in the solid state by X-ray crystallography (Fig. 8). It was clear that the [2 + 2] macrocycle H₄L had been expanded to the new 39-membered [3 + 3] macrocycle H₆L¹ on reaction with Zn(OAc)₂. As with the Ni and Cd complexes described above, the Zn^{II} ions are bound to the macrocycle solely through the imine nitrogens and the coordination spheres are completed by acetate groups. The macrocycle itself is not planar as the flexibility at the dipyrromethane *meso*-carbons promotes an overall wedge-shape in which three acetate groups are *endo*- to the cleft with the remainder *exo*. As with the free [2 + 2] ligands, this wedged conformation is stabilised by intra- and intermolecular hydrogen-bonding interactions, in this case between the oxygen atoms of the acetate groups and the acidic protons of both the pyrrolic groups and chloroform solvent of crystallisation. It is clear that the strength and number of these hydrogen-bonding interactions are implicated in the formation and unusual stability of this [3 + 3] macrocyclic complex.

The free ligand H₆L¹ was accessible from the Zn complex by reaction with Na₂S and, although stable in the solid state, contracted back to the [2 + 2] macrocycle in solution. Some insight into the structures and relative stabilities of the [2 + 2] and [3 + 3] macrocycles was gained from MMFF conformational calculations that showed that while both macrocycles adopt global minimum conformations of similar

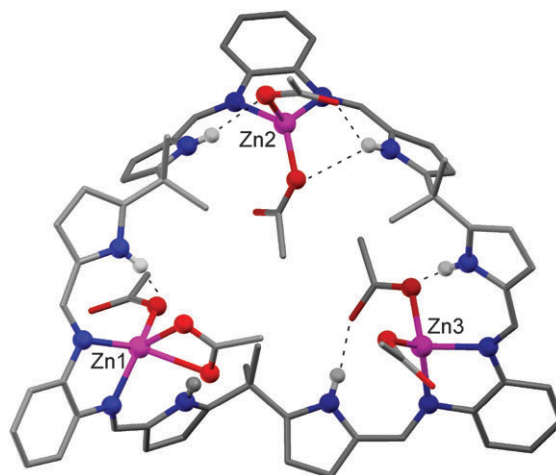


Fig. 8 Structure of a zinc acetate complex of the expanded [3 + 3] macrocycle H₆L¹.

energy, H_6L^1 adopts a more twisted conformation that, as a consequence, may result in its lack of stability with respect to contraction. In a similar manner, giant porphyrinoids have been shown to adopt twisted figure-of-eight conformations in the solid state, and have a tendency to react at the “twist” to form spirocycles or even to cleave into two separate porphyrinic products.⁴³ Furthermore, [4 + 4] to [2 + 2] macrocycle contraction has been observed during transmetallation reactions of a large, $Pb_2[4 + 4]$ Schiff-base macrocyclic complex; in this case, it is evident that coordination to the large Pb^{II} ions stabilises the twisted configuration of the [4 + 4] macrocycle.^{15,44}

Accessing early transition metal chemistry

Monometallic complexes of Groups 4, 5, and 6 have proved exceptionally versatile in the cooperative binuclear reduction and transformation of N_2 .^{5,45} However, as non-fragmentary strategies to N_2 transformation using binucleating ligands are limited to Ru cofacial diporphyrins,¹² we sought access to binuclear Pacman complexes of Ti, Zr, and V of L through the use of traditional salt elimination methods; this necessitated the synthesis of alkali-metal complexes of L.

Alkali-metal complexes

The deprotonation of H_4L by KH in THF resulted in the clean formation of the potassium salt, K_4L , in good yield.⁴⁶ The 1H NMR spectrum of K_4L in d_5 -pyridine revealed, significantly, the presence of two *meso*-methyl proton environments in K_4L that suggests that a cleft structure is favoured in solution; similar NMR characteristics were observed in the solution structures of the binuclear Pacman complexes $[Pd_2(L)]$. In the solid state, K_4L was found to crystallise as a 1D chain with a repeat unit of general formula, $[\{K_4(\mu:\kappa^2\text{-THF})(THF)_2(L)\}_\infty]$ (Fig. 9). As suggested by the NMR data, K_4L does indeed display a Pacman motif in the solid state in which the *meso*-methyl groups are *exo*- and *endo*- to the molecular cleft created by the hinged macrocycle. The presence of the THF molecule that bridges the two K1 cations causes the aryl-hinges to splay out and disrupts the π -stacking interactions between the *o*-aryl rings; this feature is also seen in uranyl complexes of this macrocycle (see below). The propensity of the pyrrolide to bind to electropositive metals in a π -fashion was also

exemplified as K_2 has a π -interaction with a pyrrole ring of an adjacent macrocycle, so causing the complex to grow as a 1D chain. This bonding motif was seen by us in the dipotassium salt of a related acyclic pyrrole-imine ligand,⁴⁷ and similar interactions were seen in alkali-metal chemistry of the porphyrinogens.⁴⁸

Ti and V complexes

The ability to generate K_4L as an isolated compound or to use it *in situ* allowed us to exploit salt elimination reactions with titanium(III) or vanadium(III) halides which were found to result in the formation of the new binuclear complexes $[(MCl)_2(L)]$ ($M = V, Ti$) in good yield. While conclusive structural data were not obtained for these complexes, the structure of the related complex $[(V=O)(THF)(VCl)(L)]$, a product of oxidation of $[(VCl)_2(L)]$, was determined (Fig. 9). Importantly, this complex adopts the desired Pacman geometry, with the vanadyl oxo-group *endo*, *i.e.* accommodated within the binuclear molecular cleft, and the chloride ligand associated with the V^{III} centre, *exo*. Both V1 and V2 adopt distorted octahedral geometries in which the V1–O1 distance of 1.652(2) Å is short and consistent with vanadyl, while the V2–O1 distance of 2.059(2) Å is considerably longer, and suggests that the vanadyl oxygen acts as a Lewis base to V2. Examples of crystallographically-characterised compounds that contain a V=O–V interaction are rare, and arise primarily from the aggregation of $[(V=O)(salen)]$ complexes and their analogues;⁴⁹ there are no examples of crystallographically-characterised mixed-valence $V^{III}V^{IV}$ -bridging vanadyl complexes. This V=O–V motif is likely a consequence of the highly-constrained Pacman geometry imposed by the macrocyclic ligand, a feature that we have observed previously in the dicopper complex $[Cu_2(py)(L)]$. Surprisingly, rational attempts to prepare a vanadyl complex of L starting from hydrated $V(O)SO_4$ were unsuccessful.

Cobalt dioxygen chemistry

Cofacial cobalt diporphyrins and their corrole relatives have been shown to manage successfully the multiple proton and electron inventories essential for the selective catalysis of the four-electron reduction of oxygen to water.^{8,28,50–54} In these compounds, the distinctive face-to-face positioning of the two metals within the diporphyrinic cleft helps circumvent routes to undesired peroxide intermediates, a feature that makes these compounds not only functional models of cytochrome *c* oxidase metalloenzymes, but also potential non-noble-metal catalysts for fuel cells. The structural similarity of compounds of cofacial diporphyrins to those of L prompted us to explore the dioxygen reduction chemistry of dicobalt compounds of L.

The anaerobic transamination reaction between anhydrous H_4L and $[Co(THF)\{N(SiMe_3)_2\}_2]$ in THF resulted in the formation of the toluene-soluble, dark red, oxygen-free $Co^{II}Co^{II}$ complex $[Co_2(L)]$ which adopts an $S = 1$ ground state derived from low-spin, square-planar $Co^{II}Co^{II}$ cations. The structure of the bis(pyridine) adduct $[Co_2(\textit{exo-py})(\textit{endo-py})(L)]$ was determined and demonstrated that a Pacman structural motif was adopted. In contrast to cobalt Pacman diporphyrins and biscorroles, the *endo*-pyridine molecule adopts a canted

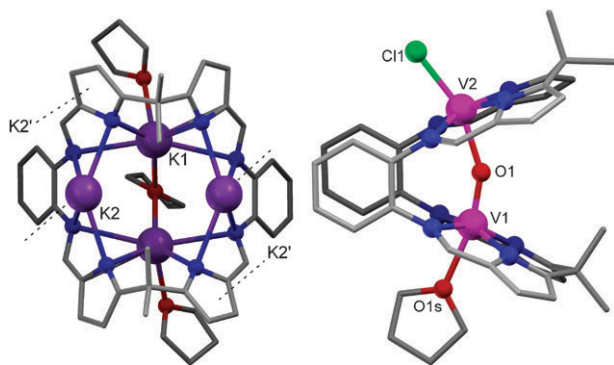


Fig. 9 Structures of the Pacman potassium salt $[\{K_4(\mu:\kappa^2\text{-THF})(THF)_2(L)\}_\infty]$ and a mixed-valence vanadyl complex $[VO(THF)VCl(L)]$.

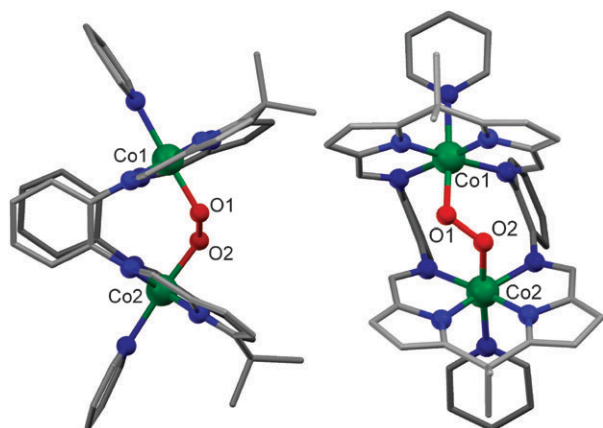


Fig. 10 Side and face-on views of the structure of the dicobalt peroxo complex $[\text{Co}_2(\text{O}_2)(\text{py})_2(\text{L})]$.

geometry ($\text{M}-\text{N}(\text{py})-\text{centroid}(\text{py}) = 162^\circ$ cf. 155° in $[\text{Cu}_2(\text{endo-py})(\text{L})]$) due to the constrained cleft environment.

The reaction between $[\text{Co}_2(\text{L})]$ and O_2 is spontaneous, and the addition of pyridine to the reaction mixture facilitated the isolation of the dioxygen complex $[\text{Co}_2(\text{O}_2)(\text{py})_2(\text{L})]$ that was characterised by X-ray crystallography (Fig. 10). It is clear from this structure that a Pacman structural motif is adopted in the solid state, and that the dioxygen ligand bridges the two cobalt centres. This is, to our knowledge, the first crystallographic characterization of O_2 bound within any dicobalt Pacman-like cleft, and correlates well to more recent *ab initio* calculations that favour Pauling $\text{Co}_2(\mu^2:\kappa^1:\kappa^1-\text{O}_2)$ coordination modes.⁵² Unfortunately, the degree of dioxygen reduction was difficult to elucidate from this structure, as the $\text{O1}-\text{O2}$ bond distance of $1.361(3)$ Å lies in-between the ranges normally associated with binuclear cobalt peroxo ($1.34\text{--}1.53$ Å, mean 1.45 Å) and superoxo complexes ($1.29\text{--}1.36$ Å; mean 1.33 Å).⁵⁵ This bond distance is also similar to that calculated for the cationic $\text{Co}^{\text{III}}\text{Co}^{\text{III}}$ superoxide $[\text{Co}_2(\mu-\text{O}_2)(\text{DPX})]^+$ at 1.35 Å.⁵² However, the lack of an anion in the X-ray structure means that it is likely that this structure represents the neutral peroxide.

In order to gain more insight into the oxygenation reactions of $[\text{Co}_2(\text{L})]$, the reaction with O_2 was monitored by EPR and ^1H NMR spectroscopy, and it was clear from these experiments that *two* products are formed: the major product $\text{Co}^{\text{III}}\text{Co}^{\text{III}}$ peroxide $[\text{Co}_2(\text{O}_2)(\text{L})]$ and the minor $\text{Co}^{\text{III}}\text{Co}^{\text{III}}$ superoxide cation $[\text{Co}_2(\text{O}_2)(\text{L})]^+$.

Indeed, the featureless fluid solution EPR spectrum of $[\text{Co}_2(\text{L})]$ in THF was found to develop into a 15-line signal under O_2 due to the formation of the superoxo radical cation $[\text{Co}_2(\mu-\text{O}_2)(\text{L})]^+$ (Fig. 11) typical of diporphyrinic analogues.^{51,53,54,56} However, quantification of the EPR signal revealed that this complex is only a minor component of the mixture ($<10\%$). In parallel NMR studies, the silent ^1H NMR spectrum of $[\text{Co}_2(\text{L})]$ in CDCl_3 was found to undergo no significant change upon exposure to O_2 , but, on addition of pyridine, an NMR spectrum due to the diamagnetic peroxo complex $[\text{Co}_2(\text{O}_2)(\text{py})_2(\text{L})]$ was seen; these features were also corroborated by *in situ* solution magnetic susceptibility measurements.

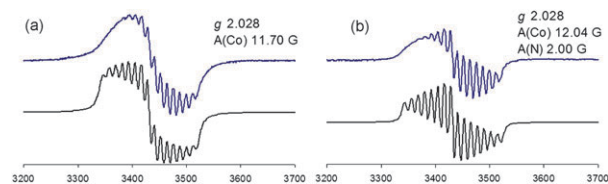


Fig. 11 Experimental (top) and simulated (bottom) EPR spectra of the superoxo complexes $[\text{Co}_2(\text{O}_2)(\text{L})]^+$ (right) and $[\text{Co}_2(\text{O}_2)(\text{py})_2(\text{L})]^+$ (left).

While the solid state structure of $[\text{Co}_2(\text{O}_2)(\text{py})_2(\text{L})]$ provides only limited insight into the degree of dioxygen reduction, it does represent a possible coordination mode of a reduced form of dioxygen within the cleft of cobalt diporphyrins. However, the oxygenation chemistry of $[\text{Co}_2(\text{L})]$ contrasts subtly to that of $[\text{Co}_2(\text{diporph})]$ complexes. While the reaction between $[\text{Co}_2(\text{L})]$ and O_2 is spontaneous and irreversible and yields, primarily, the neutral $\text{Co}^{\text{III}}\text{Co}^{\text{III}}$ peroxo complexes, $[\text{Co}_2(\text{O}_2)(\text{py})_2(\text{L})]$, the $\text{Co}^{\text{II}}\text{Co}^{\text{III}}$ diporphyrinic analogue $[\text{Co}_2(\text{diporph})]$ must first be oxidised to the $\text{Co}^{\text{II}}\text{Co}^{\text{III}}$ cation $[\text{Co}_2(\text{diporph})]^+$ before any appreciable dioxygen uptake occurs; this facilitates the reversible generation of the $\text{Co}^{\text{III}}\text{Co}^{\text{III}}$ superoxo cation $[\text{Co}_2(\text{O}_2)(\text{diporph})]^+$.⁵⁴ In our case, the formation of the superoxo complex $[\text{Co}_2(\text{O}_2)(\text{L})]^+$ would require oxidation of $[\text{Co}_2(\text{L})]$ to $[\text{Co}_2(\text{L})]^+$ prior to dioxygen binding, which would then be an entry point into the analogous porphyrinic catalytic O_2 reduction cycle. Furthermore, spontaneous dioxygen uptake by $[\text{Co}_2(\text{diporph})]$ only occurs in the presence of an imidazole base (NMeIm) and yields the $\text{Co}^{\text{III}}\text{Co}^{\text{III}}$ peroxo-bridged $[\text{Co}_2(\text{O}_2)(\text{NMeIm})_2(\text{diporph})]^+$ cation.⁵³

We have, as yet, been unable to separate the $\text{Co}^{\text{III}}\text{Co}^{\text{III}}$ superoxo cation from the peroxide. However, it is clear that facile electron transfer processes can operate during the oxygenation of $[\text{Co}_2(\text{L})]$, and that these resemble the well-studied cobalt diporphyrins.

Oxo-group chemistry of the uranyl dication

The uranyl dication, $[\text{UO}_2]^{2+}$, is the most prevalent form of uranium and is a soluble and problematic environmental contaminant. Due to the mutually-strengthening, strongly covalent *trans*- UO_2 bonding,⁵⁷ it is also extraordinarily chemically robust and shows little propensity to participate in the myriad of oxo-group and redox reactions that are characteristic of $[\text{CrO}_2]^{2+}$, $[\text{MoO}_2]^{2+}$, and other transition metal analogues.^{58–60} As a result, there are few examples in which the oxo-groups of $[\text{UO}_2]^{2+}$ are functionalised, and, despite the importance of reductive protonolysis reactions of the $[\text{UO}_2]^{2+}$ cation to its precipitation from the environment, the isolation and characterisation of the singly-reduced, pentavalent uranyl cation $[\text{UO}_2]^+$ complexes have only recently been reported.^{61,62}

We reasoned that the large and flexible macrocycle H_4L should be able to accommodate the uranyl dication in a way that binucleating, cofacial diporphyrin ligands cannot, and that the tendency of this ligand set to promote hinged, ‘Pacman’ geometries could be exploited to study the oxo chemistry of the uranyl ion.

Uranyl complexes

Indeed, the transamination reaction between H₄L and the uranyl amide [UO₂(THF)₂{N(SiMe₃)₂}₂] in THF resulted in the rapid and sole formation of the mono-uranyl complex, *trans*-[UO₂(THF)(H₂L)]. Significantly, no diuranyl complex was observed, even when the reaction was carried out at elevated temperature.

In the X-ray crystal structure (Fig. 12), it was immediately evident that one N₄-donor compartment of macrocycle had expanded sufficiently to accommodate the *trans*-uranyl ion and that the second N₄-donor compartment remains metal-free. The THF molecule in the 5th equatorial site adopts a highly unusual, “sandwiched” position between the two aryl rings that bridge the two N₄-donor compartments and this coordination mode results in a significantly more obtuse N1–M–N4 angle than that seen in [Pd₂(L)] (150.74(16)° *cf.* 110.93(12)°). Even though the macrocycle has flexed considerably to accommodate one uranyl ion and π – π stacking between the two aryl ring hinges has been lost, the overall molecular topology is still remarkably similar to transition metal Pacman complexes supported by L, and prescribes a well-defined, monometallic cleft with one oxo-group of the linear uranyl ion located within the cleft and the other *exo*. Furthermore, this geometry directs an appreciable hydrogen-bonding interaction between the pyrrolic hydrogens and the *endo*-uranyl oxygen O1 which results in elongation of the U1–O1 bond distance as compared to U1–O2 (by 0.024 Å), *i.e.* the uranyl has been desymmetrised. Building-in hydrogen-bonding sites into the ligand design has been shown to stabilise reactive intermediates and to enhance catalytic activity.³⁸ As with other [M₂(L)] complexes, this solid state structure is retained in solution with discrete resonances seen for both complexed and metal-free N₄-compartments, and also for the asymmetric THF molecule in the ¹H NMR spectrum.

Cation–cation complexes

Actinyl complexes that display Lewis base interactions between the oxo and a metal counterion, *i.e.* AnO₂²⁺...M⁺, so-called cation–cation complexes, are important species in neptunium and plutonium chemistry.⁶³ However, the relative inertness of the [UO₂]²⁺ congenor means that there are very few simple, molecular uranyl-based cation–cation complexes.⁶⁴ These uranyl analogues would be desirable for

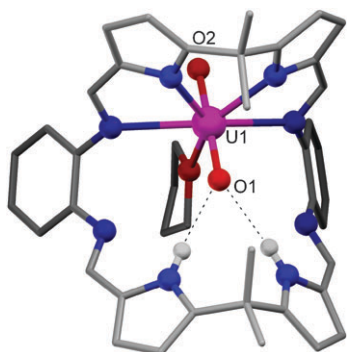


Fig. 12 Complexation and desymmetrisation of the uranyl dication in [UO₂(THF)(H₂L)].

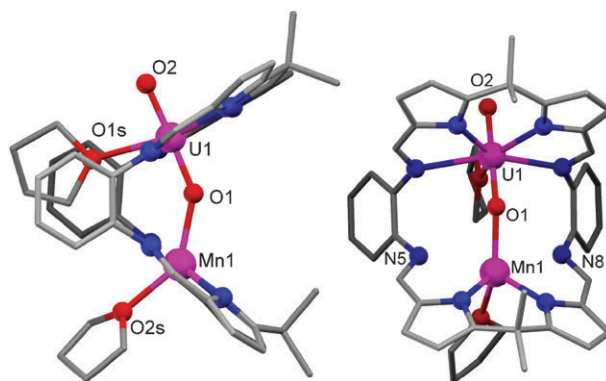


Fig. 13 Side and face-on views of the structure of the uranyl cation–cation complex [UO₂(THF)Mn(THF)(L)].

understanding the speciation of the highly radioactive metals in nuclear fuel processing and the environment. Furthermore, of the handful of uranyl cation–cation complexes which form in the solid state, none are retained in solution. We reasoned that the ready formation of the mono-uranyl complex [UO₂(THF)(H₂L)] with its vacant N₄-donor compartment would enable us to study the formation of new uranyl cation–cation complexes.

Indeed, transamination reactions between the mono-uranyl complex [UO₂(THF)(H₂L)] and the low-coordinate metal amides [M{N(SiMe₃)₂}₂] (M = Mn, Fe, Co) in boiling THF afforded the brown cation–cation complexes [UO₂(THF)M(THF)(L)]. Unlike other cation–cation complexes of the uranyl dication, these are neutral, and undergo neither metal exchange nor redistribution reactions in solution; the electrospray mass spectrum of [UO₂(THF)Fe(THF)(L)] in THF displays a parent ion for [M + Na]⁺. The solid state structures (Fig. 13, M = Mn) for [UO₂(THF)M(THF)(L)] (M = Mn, Fe) are isostructural and demonstrate interaction between the uranyl oxo atom and a transition metal for the first time. Significantly, these transition metal cations are common in both minerals and uranium wastes, and iron is often implicated in uranyl reduction chemistry in vitrified materials and geological samples.⁶⁵ The most striking feature of the structure is the transition metal to uranyl-oxygen bond that is formed within the cavity, resulting in a Mn1–O1 single bond distance of 2.163(4) Å, and a corresponding lengthening of the U=O1 bond to 1.808(4) Å from 1.790(4) Å in [UO₂(THF)(H₂L)]. There are no other transition metal–oxo–uranyl complexes reported with which to compare this bond distance, although the polyoxometallate adduct of [¹³⁷Bu₄N]₄[Mn(OH₂)₂{(μ-O)₂Mo₅O₁₄(OMe)₂}₂{Mn(CO)₃}₂] displays four Mn–oxo distances that range between 2.13(2) and 2.18(2) Å.⁶⁶

The manganese ion is not a particularly good fit for the bottom cavity, and adopts a pseudo-tetrahedral geometry by bonding to the two pyrrolide nitrogens, the *endo*-uranyl oxo and a molecule of THF; only weak interactions to the two imino N atoms occur, presumably as a consequence of the π -stacked THF on the uranyl ion causing the aryl hinge to ‘open’. The U–N and Mn–N pyrrolide distances are normal for U^{VI} and Mn^{II}, and so suggest that the metal oxidation

states remain unchanged. This lack of redox chemistry is reinforced by magnetic susceptibility measurements for $[\text{UO}_2(\text{THF})\text{M}(\text{THF})(\text{L})]$ which have been studied in the solid state by SQUID magnetometry and are fitted very well by models which assume $\text{U}^{\text{VI}}\text{M}^{\text{II}}$ oxidation states with high-spin configurations for the transition metal cations, and Curie–Weiss paramagnetic behaviour. While the IR and Raman spectra of $[\text{UO}_2(\text{THF})\text{M}(\text{THF})(\text{L})]$ are complicated by overlapping ligand absorptions, the $\text{U}=\text{O}$ asymmetric stretch is seen between 811 and 804 cm^{-1} , which is $\sim 65\text{ cm}^{-1}$ lower than in the simplest uranyl aquo complex $[\text{UO}_2(\text{OH}_2)_5]^{2+}$.⁶⁷

Calculations

In order to probe the $\text{O}=\text{U}=\text{O}-\text{M}$ bonding further and extrapolate our experimental results to the heavier actinyls, density functional calculations were carried out by Schreckenbach and co-workers on the series of cation–cation compounds $[\text{MO}_2(\text{THF})\text{M}'(\text{THF})(\text{L})]$ ($\text{M} = \text{U}, \text{Np}, \text{Pu}$; $\text{M}' = \text{Mn}, \text{Fe}, \text{Co}, \text{Zn}$).⁶⁸ These data showed that the *endo*-O to transition metal bond order varied between 0.36 and 0.81 , with the strongest bonds associated with Fe and Pu. As such, these data support the increased prevalence of cation–cation interactions with the heavier actinyls which show greater oxo-group reactivity than the uranyl dication. The $\text{An}^{\text{VI}/\text{V}}$ redox couple was also probed and showed the trend $\text{U} \gg \text{Np} > \text{Pu}$, with the calculated $\text{U}^{\text{VI}/\text{V}}$ redox couple being only slightly lower than that observed experimentally (-1.10 *cf.* -1.18 V).

Reductive silylation of $[\text{UO}_2]^{2+}$

Reactions of the uranyl dication that result in the functionalisation or transformation of the $\text{U}=\text{O}$ groups are rare. Atypical Lewis base behaviour of the uranyl dioxo-group towards alkali-metals has been observed in the solid state, and in the formation of an unusual $\text{O}=\text{U}=\text{O}\cdot\text{B}(\text{C}_6\text{F}_5)_3$ adduct in which significant, and asymmetric, $\text{U}=\text{O}$ bond lengthening was seen.⁶⁹ Photolysis of uranyl phosphine oxide complexes in the presence of alcohols has been shown to result in two-electron reduction and the formation of $\text{U}(\text{IV})$ alkoxides, *via* the highly oxidising $^*\text{UO}_2^{2+}$ excited state; the $\text{U}(\text{IV})$ complexes can be hydrolysed to regenerate cleanly the uranyl dication.⁷⁰

While our transamination synthetic route to uranyl–transition metal cation–cation complexes was efficient, we thought that a salt elimination strategy, in which the vacant N_4 -compartment is first deprotonated prior to reaction with a metal halide, would allow us to introduce more reducing metals. However, we instead found that the one-pot reaction between $[\text{UO}_2(\text{THF})(\text{H}_2\text{L})]$, MI_2 ($\text{M} = \text{Fe}, \text{Zn}$), and the silylamide base $\text{KN}(\text{SiMe}_3)_2$ resulted in the formation of the new cation–cation complex $[\text{UO}(\text{OSiMe}_3)(\text{THF})\text{M}_2\text{I}_2(\text{L})]$ in 80% yield.⁷¹

The X-ray crystal structures determined for $\text{M} = \text{Fe}$ and Zn are isostructural (Fig. 14, Zn shown) and showed that the macrocycle geometry remained wedge-shaped, even though *two* tetrahedral M^{2+} cations were now incorporated in the lower cavity, and a Me_3Si group was bound to the *exo*-uranyl oxygen. As with our previous macrocyclic uranyl complexes,

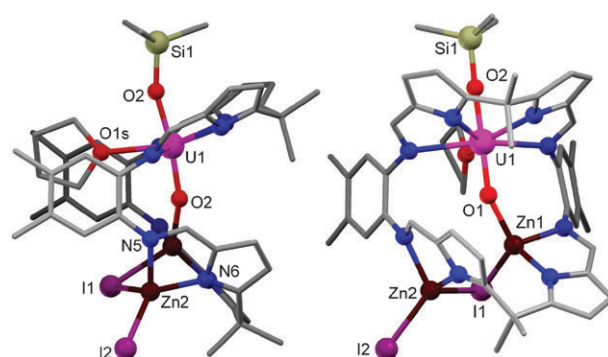


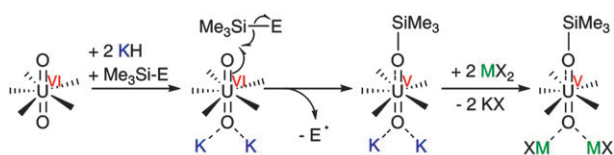
Fig. 14 Side and face-on views of the reductively functionalised uranyl(v) complex $[\text{UO}(\text{OSiMe}_3)(\text{THF})\{\text{ZnI}_2\}(\text{L})]$ (*n.b.* L derived from dimethyl-*o*-phenylenediamine).

the uranyl cation adopted a distorted pentagonal bipyramidal geometry with a linear $\text{O1}-\text{U1}-\text{O2}$ group. However, the $\text{U}-\text{O}$ bond distances in the silylated complexes support a pentavalent oxidation state. For example, the *endo*- $\text{U1}-\text{O1}$ ($1.870(4)\text{ \AA}$, $\text{M} = \text{Fe}$) bond distance is similar to experimental and calculated bond distances for pentavalent $[\text{UO}_2]^+$ (range 1.811 to 1.934 \AA),^{62,72} and the *exo*- $\text{U1}-\text{O2}$ ($1.993(4)\text{ \AA}$, $\text{M} = \text{Fe}$) bond distance, while appreciably longer, is significantly shorter than that seen in tetravalent $\text{U}-\text{OSiR}_3$ and pentavalent $\text{U}-\text{OR}$ compounds (all $> 2.0\text{ \AA}$).⁷³ This therefore implied that the *exo*- $\text{U}-\text{O}$ bond still retains some multiple bond character, but less than that of the *endo*- $\text{U}-\text{O}$ bond. Both transition metal cations are four-coordinate and bound to the macrocycle by single iminopyrrolidate, and to each other by a bridging iodide, with one metal bound to the *endo*-uranyl oxygen at a distance commensurate with a single dative bond. From these structural data, it was clear that the uranyl dication had undergone reductive silylation.

Mechanistic investigations

A series of experiments were carried out to probe the origin of the SiMe_3 group and to confirm the single-electron transfer to form pentavalent uranyl. In the first instance, the use of the silylamide base $\text{KN}(\text{SiMe}_2\text{Ph})_2$ afforded the phenylsilyl-functionalised $[\text{UO}(\text{OSiMe}_2\text{Ph})(\text{THF})\text{Fe}_2\text{I}_2(\text{L})]$ in high yield. As a consequence, it was clear that the silyl group originated from either the silylamide base, $\text{KN}(\text{SiMe}_2\text{R})_2$, or its by-product, the disilazane $\text{HN}(\text{SiMe}_2\text{R})_2$ ($\text{R} = \text{Me}, \text{Ph}$). Analysis of the mass balance for the by-product KI showed that two molar equivalents were formed during the reaction, and implied that electron transfer from $\text{KN}(\text{SiMe}_2\text{R})_2$ did not occur, *i.e.* the silylamide acts solely as a base, and the $\text{HN}(\text{SiMe}_2\text{R})_2$ by-product formed during the reaction provides the silyl group. In contrast, transition metal analogues, the molybdenum and tungsten *cis*-dioxo complexes $[\text{M}^{\text{VI}}\text{O}_2(\text{L})_2]^{2-}$ ($\text{M} = \text{Mo}, \text{W}$; $\text{L} = 1,2\text{-S}_2\text{C}_6\text{H}_4$), are readily silylated, even in the absence of redox reactions, to afford $[\text{M}^{\text{VI}}\text{O}(\text{OSiMe}_2\text{Bu}^t)(\text{L})_2]^-$. Furthermore, the silylated Mo compound is rapidly hydrolysed to the $\text{Mo}(\text{IV})$ mono-oxo compound $[\text{Mo}^{\text{IV}}\text{O}(\text{L})_2]^{2-}$.⁷⁴

With the isolation of the closed-shell $\text{Zn}(\text{II})$ compounds, it was also clear that the transition metal simply stabilises the pentavalent $[\text{UO}(\text{OSiMe}_2\text{R})]^+$ fragment, without participating



Scheme 2 Proposed mechanism for the base-assisted reductive silylation of the uranyl dication.

in redox chemistry. Furthermore, treatment of [UO₂(THF)(H₂L)] with a reductant (rather than a base), and a source of SiMe₃, in these cases cobaltocene and trimethylsilyl triflate, did not result in reductive silylation. Knowing this, we began to generalise the reaction further, and found that the potassium silylamide may be replaced by potassium hydride in combination with other sources of silyl group. Thus, reaction with KH and either N(SiMe₃)₃ or PhCH₂SiMe₃ proved equally effective in this reductive silylation chemistry, affording isolated yields of [UO(OSiMe₃)⁺ complexes of up to 85%, via N–Si or C–Si bond cleavage.

These data suggested that this reaction requires initially the deprotonation of the empty macrocyclic cavity by the potassium base to form potentially an oxidising, U^{VI}, intermediate in which the *endo*-U=O bond is coordinated by two K cations, and the *exo*-U=O bond is now polarised sufficiently to engage in N–Si and C–Si bond cleavage (Scheme 2). Very recently, Maron and co-workers have carried out density functional calculations on model uranyl macrocyclic complexes to probe theoretically the mechanism of this reaction.⁷⁵ These results correlate well with our proposed mechanism and show that the radical reaction proceeds through an S_N2-type transition state and is driven downhill thermodynamically by up to 148 kcal mol⁻¹ by initial reaction with two equivalents of potassium base. Significantly, both potassium cations are found to coordinate to the same oxo-group which leaves the opposing oxo-group free to participate in silane bond cleavage chemistry.

This reaction provides an actinyl parallel to well-known transition metal chemistry. In high oxidation state porphyrin-based iron oxo chemistry, tuning the axial ligand has been shown to alter markedly the reactivity of the electrophilic Fe=O group towards alkane hydroxylation and olefin epoxidation.⁶⁰ Likewise, by manipulating the uranyl oxo within the molecular cleft, it is apparent that we have disrupted significantly the overall UO₂ bonding and that this activates the *exo*-oxo-group towards reductive silylation. Furthermore, the ready formation of strong O–Si bonds is similar to that seen in transition metal oxo chemistry in which hydrogen atom abstraction reactions do not require metal-based radicals, but instead depend on the strength of the bond between the oxidant and the hydrogen atom.⁵⁹

Summary and outlook

The straightforwardly synthesised Schiff-base polypyrrolic macrocycles described in this article have allowed the formation of a variety of shape-persistent transition metal and f-element complexes. In the main, binuclear complexes of

these macrocycles are ‘Pacman’-shaped and reminiscent of cofacial or Pacman diporphyrin complexes. Even so, alternative, bowl-shaped structures can be generated in which extensive hydrogen-bonding interactions are evident. Similarities exist between Pacman porphyrins and these calixpyrrole analogues, in particular in the dioxygen chemistry of binuclear cobalt complexes. However, the lateral rigidity of the cleft, the flexibility of the pyrrole-imine chelates, and the ready expansion of the N₄-donor cavity has facilitated, in particular, new oxo-group chemistry of the uranyl dication that would not be possible using the porphyrinic analogues.

The modular synthetic approach to these macrocyclic ligands should mean that they are easily tailored to provide a diversity of shape, size and redox and metal complexation properties, which makes them applicable to a host of current chemistry themes, such as molecular recognition, metal value extraction/sequestration, asymmetric synthesis, medicinal inorganic chemistry, capsular self-assembly processes, and multinuclear redox chemistry.

Acknowledgements

JBL thanks the Royal Society, EPSRC (UK), The Nuffield Foundation, and the Universities of Sussex, Nottingham, and Edinburgh for funding. JBL is indebted to all past and present co-workers who have contributed enormously to this work, and in particular for fruitful collaborations with Prof. Martin Schröder (Nottingham), and Dr Polly Arnold (Nottingham and Edinburgh).

Notes and references

- R. Eisenberg and H. B. Gray, *Inorg. Chem.*, 2008, **47**, 1697; M. W. Kanan and D. G. Nocera, *Science*, 2008, **321**, 1072; X. Sala, I. Romero, M. Rodriguez, L. Escriche and A. Llobet, *Angew. Chem., Int. Ed.*, 2009, **48**, 2842; K. N. Ferreira, T. M. Iverson, K. Maghlaoui, J. Barber and S. Iwata, *Science*, 2004, **303**, 1831.
- R. Bashyam and P. Zelenay, *Nature*, 2006, **443**, 63; B. Wang, *J. Power Sources*, 2005, **152**, 1.
- J. L. Dempsey, A. J. Esswein, D. R. Manke, J. Rosenthal, J. D. Soper and D. G. Nocera, *Inorg. Chem.*, 2005, **44**, 6879; N. S. Lewis and D. G. Nocera, *Proc. Natl. Acad. Sci. U. S. A.*, 2006, **103**, 15729.
- J. P. Collman, R. Boulatov, C. J. Sunderland and L. Fu, *Chem. Rev.*, 2004, **104**, 561; J. P. Collman, L. Fu, P. C. Herrmann and X. Zhang, *Science*, 1997, **275**, 949; D. J. Evans and C. J. Pickett, *Chem. Soc. Rev.*, 2003, **32**, 268; D. J. E. Spencer, A. C. Marr and M. Schröder, *Coord. Chem. Rev.*, 2001, **219–221**, 1055; R. H. Holm, P. Kennepohl and E. I. Solomon, *Chem. Rev.*, 1996, **96**, 2563; B. A. MacKay and M. D. Fryzuk, *Chem. Rev.*, 2004, **104**, 385.
- M. D. Fryzuk and S. A. Johnson, *Coord. Chem. Rev.*, 2000, **200–202**, 379.
- B. Bosnich, *Inorg. Chem.*, 1999, **38**, 2554; J. Du Bois, T. J. Mizoguchi and S. J. Lippard, *Coord. Chem. Rev.*, 2000, **200–202**, 443; A. L. Gavrilova and B. Bosnich, *Chem. Rev.*, 2004, **104**, 349; G. Rowlands, *Tetrahedron*, 2001, **57**, 1865; E. K. van den Beuken and B. L. Feringa, *Tetrahedron*, 1998, **54**, 12985.
- J. P. Collman, P. S. Wagenknecht and J. E. Hutchinson, *Angew. Chem., Int. Ed. Engl.*, 1994, **33**, 1537.
- J. Rosenthal and D. G. Nocera, *Prog. Inorg. Chem.*, 2007, **55**, 483; J. Rosenthal and D. G. Nocera, *Acc. Chem. Res.*, 2007, **40**, 543.
- P. D. Harvey, C. Stern, C. P. Gros and R. Guillard, *Coord. Chem. Rev.*, 2007, **251**, 401.

- 10 J. Rosenthal, T. D. Lockett, J. M. Hodgkiss and D. G. Nocera, *J. Am. Chem. Soc.*, 2006, **128**, 6546; J. Rosenthal, B. J. Pistorio, L. L. Chng and D. G. Nocera, *J. Org. Chem.*, 2005, **70**, 1885.
- 11 J. P. Collman, H. T. Fish, P. S. Wagenknecht, D. A. Tyvoll, L.-L. Chng, T. A. Eberspacher, J. I. Brauman, J. W. Bacon and L. H. Pignolet, *Inorg. Chem.*, 1996, **35**, 6746; J. P. Collman, J. E. Hutchison, P. S. Wagenknecht, N. S. Lewis, M. A. Lopez and R. Guilard, *J. Am. Chem. Soc.*, 1990, **112**, 8206.
- 12 J. P. Collman, J. E. Hutchison, M. S. Ennis, M. A. Lopez and R. Guilard, *J. Am. Chem. Soc.*, 1992, **114**, 8074; J. P. Collman, J. E. Hutchison, M. A. Lopez and R. Guilard, *J. Am. Chem. Soc.*, 1992, **114**, 8066; J. P. Collman, J. E. Hutchison, M. A. Lopez, R. Guilard and R. A. Reed, *J. Am. Chem. Soc.*, 1991, **113**, 2794.
- 13 W. Cui and B. B. Wayland, *J. Am. Chem. Soc.*, 2004, **126**, 8266; W. Cui, X. P. Zhang and B. B. Wayland, *J. Am. Chem. Soc.*, 2003, **125**, 4994; X.-X. Zhang and B. B. Wayland, *Inorg. Chem.*, 2000, **39**, 5318.
- 14 W. B. Callaway, J. M. Veauthier and J. L. Sessler, *J. Porphyrins Phthalocyanines*, 2004, **8**, 1; P. A. Vigato, S. Tamburini and L. Bertolo, *Coord. Chem. Rev.*, 2007, **251**, 1311; W. Radecka-Paryzek, V. Patroniak and J. Lisowski, *Coord. Chem. Rev.*, 2005, **249**, 2156; R. Hernandez-Molina and A. Mederos, in *Comprehensive Organometallic Chemistry II*, Elsevier Ltd., Oxford, 2004; A. C. W. Leung and M. J. MacLachlan, *J. Inorg. Organomet. Polym. Mater.*, 2007, **17**, 57; M. J. MacLachlan, *Pure Appl. Chem.*, 2006, **78**, 873.
- 15 S. Brooker, *Eur. J. Inorg. Chem.*, 2002, 2535.
- 16 C. Floriani, *Chem. Commun.*, 1996, 1257; I. Korobkov, S. Gambarotta and G. P. A. Yap, *Angew. Chem., Int. Ed.*, 2002, **41**, 3433.
- 17 P. A. Gale, P. Anzenbacher Jr. and J. L. Sessler, *Coord. Chem. Rev.*, 2001, **222**, 57.
- 18 T. D. Mody and J. L. Sessler, *J. Porphyrins Phthalocyanines*, 2001, **5**, 134.
- 19 J. L. Sessler, A. E. Vivian, D. Seidel, A. K. Burrell, M. Hoehner, T. D. Mody, A. Gebauer, S. J. Weghorn and V. Lynch, *Coord. Chem. Rev.*, 2001, **216–217**, 411.
- 20 G. Givaja, A. J. Blake, C. Wilson, M. Schröder and J. B. Love, *Chem. Commun.*, 2003, 2508.
- 21 G. Givaja, M. Volpe, J. W. Leeland, M. A. Edwards, T. K. Young, S. B. Darby, S. D. Reid, A. J. Blake, C. Wilson, J. Wolowska, E. J. L. McInnes, M. Schröder and J. B. Love, *Chem.–Eur. J.*, 2007, **13**, 3707.
- 22 N. E. Borisova, M. D. Reshetova and Y. A. Ustyniyuk, *Chem. Rev.*, 2007, **107**, 46.
- 23 J. L. Sessler, W.-S. Cho, S. P. Dudek, L. Hicks, V. M. Lynch and M. T. Huggins, *J. Porphyrins Phthalocyanines*, 2003, **7**, 97.
- 24 J. L. Sessler, S. Cambiolo and P. A. Gale, *Coord. Chem. Rev.*, 2003, **240**, 17.
- 25 D. Dolphin and A. Jasat, *Chem. Rev.*, 1997, **97**, 2267; J. L. Sessler and D. Seidel, *Angew. Chem., Int. Ed.*, 2003, **42**, 5134.
- 26 Y. Deng, C. J. Chang and D. G. Nocera, *J. Am. Chem. Soc.*, 2000, **122**, 410.
- 27 Z.-H. Loh, S. E. Miller, C. J. Chang, S. D. Carpenter and D. G. Nocera, *J. Phys. Chem. A*, 2002, **106**, 11700.
- 28 Y. Shimazaki, H. Takesue, T. Chishiro, F. Tani and Y. Naruta, *Chem. Lett.*, 2001, 539.
- 29 A. Osuka, S. Nakajima, T. Nagata, K. Maruyama and K. Toriumi, *Angew. Chem., Int. Ed. Engl.*, 1991, **30**, 582.
- 30 J. M. Veauthier, W.-S. Cho, V. M. Lynch and J. L. Sessler, *Inorg. Chem.*, 2004, **43**, 1220.
- 31 W. A. Reiter, A. Gerges, S. Lee, T. Deffo, T. Clifford, A. Danby and K. Bowman-James, *Coord. Chem. Rev.*, 1998, **174**, 343.
- 32 R. Li, T. A. Mulder, U. Beckmann, P. D. W. Boyd and S. Brooker, *Inorg. Chim. Acta*, 2004, **357**, 3360.
- 33 J. M. Veauthier, E. Tomat, V. M. Lynch, J. L. Sessler, U. Mirsaidov and J. T. Markert, *Inorg. Chem.*, 2005, **44**, 6736.
- 34 E. C. Constable, A. J. Edwards, M. J. Hannon and P. R. Raithby, *J. Chem. Soc., Chem. Commun.*, 1994, 1991; E. C. Constable, T. Kulke, M. Neuburger and M. Zehnder, *Chem. Commun.*, 1997, 489; M. G. B. Drew, A. Lavery, V. McKee and S. M. Nelson, *J. Chem. Soc., Dalton Trans.*, 1985, 1771; C. Piguet, G. Bernardinelli and A. F. Williams, *Inorg. Chem.*, 1989, **28**, 2920; K. T. Potts, M. Keshavarz, F. S. Tham, H. D. Abruna and C. Arana, *Inorg. Chem.*, 1993, **32**, 4450;
- T. Yano, R. Tanaka, I. Kinoshita, K. Isobe, L. J. Wright and T. J. Collins, *Chem. Commun.*, 2002, 1396.
- 35 C. J. Chang, Z.-H. Loh, Y. Deng and D. G. Nocera, *Inorg. Chem.*, 2003, **42**, 8262.
- 36 D. Jokic, C. Boudon, G. Pognon, M. Bonin, K. J. Schenk, M. Gross and J. Weiss, *Chem.–Eur. J.*, 2005, **11**, 4199; S. Yagi, M. Ezoe, I. Yonekura, T. Takagishi and H. Nakazumi, *J. Am. Chem. Soc.*, 2003, **125**, 4068.
- 37 D. Sun, F. S. Tham, C. A. Reed, L. Chaker, M. Burgess and P. D. W. Boyd, *J. Am. Chem. Soc.*, 2000, **122**, 10704.
- 38 A. S. Borovik, *Acc. Chem. Res.*, 2005, **38**, 54; D. Natale and J. C. Mareque-Rivas, *Chem. Commun.*, 2008, 425; R. L. Shook and A. S. Borovik, *Chem. Commun.*, 2008, 6095.
- 39 G. Givaja, A. J. Blake, C. Wilson, M. Schroder and J. B. Love, *Chem. Commun.*, 2005, 4423.
- 40 L. Cuesta, E. Tomat, V. M. Lynch and J. L. Sessler, *Chem. Commun.*, 2008, 3744.
- 41 E. Tomat, L. Cuesta, V. M. Lynch and J. L. Sessler, *Inorg. Chem.*, 2007, **46**, 6224.
- 42 J. R. Nitschke, *Acc. Chem. Res.*, 2007, **40**, 103.
- 43 T. D. Lash, *Angew. Chem., Int. Ed.*, 2000, **39**, 1763; L. Latos-Grażyński, *Angew. Chem., Int. Ed.*, 2004, **43**, 5124.
- 44 S. Brooker and R. J. Kelly, *J. Chem. Soc., Dalton Trans.*, 1996, 2117.
- 45 M. P. Shaver and M. D. Fryzuk, *Adv. Synth. Catal.*, 2003, **345**, 1061.
- 46 M. Volpe, S. D. Reid, A. J. Blake, C. Wilson and J. B. Love, *Inorg. Chim. Acta*, 2007, **360**, 273.
- 47 S. D. Reid, A. J. Blake, C. Wilson and J. B. Love, *Inorg. Chem.*, 2006, **45**, 636.
- 48 L. Bonomo, E. Solari, R. Scopelliti and C. Floriani, *Chem.–Eur. J.*, 2001, **7**, 1322.
- 49 S. A. Fairhurst, D. L. Hughes, G. J. Leigh, J. R. Sanders and J. Weisner, *J. Chem. Soc., Dalton Trans.*, 1995, 321; B. A. Goodman and J. B. Raynor, *Adv. Inorg. Chem. Radiochem.*, 1970, **13**, 136; D. L. Hughes, U. Kleinkes, G. J. Leigh, M. Maiwald, J. R. Sanders and C. Sudbrake, *J. Chem. Soc., Dalton Trans.*, 1994, 2457; K. Nakajima, M. Kojima, S. Azuma, R. Kasahara, M. Tsuchimoto, Y. Kubozono, H. Maeda, S. Kashino, S. Ohba, Y. Yoshikawa and J. Fujita, *Bull. Chem. Soc. Jpn.*, 1996, **69**, 3207; K. K. Nanda, S. Mohanta, S. Ghosh, M. Mukherjee, M. Helliwell and K. Nag, *Inorg. Chem.*, 1995, **34**, 2861; W. Tsagkalidis and D. Rehder, *J. Biol. Inorg. Chem.*, 1996, **1**, 507; E. Tsuchida and K. Oyaizu, *J. Am. Chem. Soc.*, 2003, **125**, 5630.
- 50 S. Fukuzumi, *Chem. Lett.*, 2008, 808; C. K. Chang, H. Y. Liu and I. Abdalmuhdi, *J. Am. Chem. Soc.*, 1984, **106**, 2725; J. P. Collman, N. H. Hendricks, C. R. Leidner, E. Ngameni and M. L'Her, *Inorg. Chem.*, 1988, **27**, 387; R. R. Durand Jr, C. S. Bencosme, J. P. Collman and F. C. Anson, *J. Am. Chem. Soc.*, 1983, **105**, 2710; S. Fukuzumi, K. Okamoto, C. P. Gros and R. Guilard, *J. Am. Chem. Soc.*, 2004, **126**, 10441; R. Guilard, S. Brandès, C. Tardieux, A. Tabard, M. L'Her, C. Miry, P. Guerec, Y. Knop and J. P. Collman, *J. Am. Chem. Soc.*, 1995, **117**, 11721; K. M. Kadish, L. Fremond, F. Burdet, J.-M. Barbe, C. P. Gros and R. Guilard, *J. Inorg. Biochem.*, 2006, **100**, 858; K. M. Kadish, L. Fremond, Z. Ou, J. Shao, C. Shi, F. C. Anson, F. Burdet, C. P. Gros, J.-M. Barbe and R. Guilard, *J. Am. Chem. Soc.*, 2005, **127**, 5625; K. M. Kadish, J. Shao, Z. Ou, L. Fremond, R. Zhan, F. Burdet, J.-M. Barbe, C. P. Gros and R. Guilard, *Inorg. Chem.*, 2005, **44**, 6744; G. J. Park, S. Nakajima, A. Osuka and K. Kim, *Chem. Lett.*, 1995, 255.
- 51 C. J. Chang, Y. Deng, C. Shi, F. C. Anson and D. G. Nocera, *Chem. Commun.*, 2000, 1355; J. P. Collman, P. Denisevich, Y. Konai, M. Marrocco, C. Koval and F. C. Anson, *J. Am. Chem. Soc.*, 1980, **102**, 6027; J. P. Collman, N. H. Hendricks, K. Kim and C. S. Bencosme, *J. Chem. Soc., Chem. Commun.*, 1987, 1537.
- 52 C. J. Chang, Z.-H. Loh, C. Shi, F. C. Anson and D. G. Nocera, *J. Am. Chem. Soc.*, 2004, **126**, 10013.
- 53 J. P. Collman, J. E. Hutchison, M. Angel Lopez, A. Tabard, R. Guilard, W. K. Seok, J. A. Ibers and M. L'Her, *J. Am. Chem. Soc.*, 1992, **114**, 9869.
- 54 Y. Le Mest, C. Inisan, A. Laouenan, M. L'Her, J. Talarmin, M. El Khalifa and J.-Y. Saillard, *J. Am. Chem. Soc.*, 1997, **119**, 6095.

- 55 D. A. Fletcher, R. F. McMeeking and D. Parkin, *J. Chem. Inf. Comput. Sci.*, 1996, **36**, 746.
- 56 C. K. Chang, *J. Chem. Soc., Chem. Commun.*, 1977, 800; Y. Le Mest and M. L'Her, *J. Am. Chem. Soc.*, 1986, **108**, 533; L. M. Proniewicz, J. Odo, J. Goral, C. K. Chang and K. Nakamoto, *J. Am. Chem. Soc.*, 1989, **111**, 2105.
- 57 R. G. Denning, *J. Phys. Chem. A*, 2007, **111**, 4125.
- 58 C. Limberg, *Angew. Chem., Int. Ed.*, 2003, **42**, 5932; F. E. Kühn, A. M. Santos and M. Abrantes, *Chem. Rev.*, 2006, **106**, 2455.
- 59 J. M. Mayer, *Acc. Chem. Res.*, 1998, **31**, 441.
- 60 W. Nam, *Acc. Chem. Res.*, 2007, **40**, 522.
- 61 G. Nocton, P. Horeglad, J. Pecaut and M. Mazzanti, *J. Am. Chem. Soc.*, 2008, **130**, 16633; T. W. Hayton and G. Wu, *J. Am. Chem. Soc.*, 2008, **130**, 2005; P. L. Arnold, J. B. Love and D. Patel, *Coord. Chem. Rev.*, 2009, DOI: 10.1016/j.ccr.2009.03.014.
- 62 J. C. Berthet, G. Siffredi, P. Thuery and M. Ephritikhine, *Chem. Commun.*, 2006, 3184; F. Burdet, J. Pecaut and M. Mazzanti, *J. Am. Chem. Soc.*, 2006, **128**, 16512; L. Natrajan, F. Burdet, J. Pecaut and M. Mazzanti, *J. Am. Chem. Soc.*, 2006, **128**, 7152.
- 63 A. E. V. Gorden, J. Xu, K. N. Raymond and P. Durbin, *Chem. Rev.*, 2003, **103**, 4207; S. D. Reilly and M. P. Neu, *Inorg. Chem.*, 2006, **45**, 1839; J. L. Sessler, A. E. V. Gorden, D. Seidel, S. Hannah, V. Lynch, P. L. Gordon, R. J. Donohoe, C. Drew Tait and D. Webster Keogh, *Inorg. Chim. Acta*, 2002, **341**, 54.
- 64 C. J. Burns, D. L. Clark, R. J. Donohoe, P. B. Duval, B. L. Scott and C. D. Tait, *Inorg. Chem.*, 2000, **39**, 5464; J. A. Danis, M. R. Lin, B. L. Scott, B. W. Eichhorn and W. H. Runde, *Inorg. Chem.*, 2001, **40**, 3389; G. H. John, I. May, M. J. Sarsfield, H. M. Steele, D. Collison, M. Helliwell and J. D. McKinney, *Dalton Trans.*, 2004, 734; M. J. Sarsfield, M. Helliwell and J. Raftery, *Inorg. Chem.*, 2004, **43**, 3170; P. Thuery, *Chem. Commun.*, 2006, 853.
- 65 T. B. Scott, G. C. Allen, P. J. Heard and M. G. Randell, *Geochim. Cosmochim. Acta*, 2005, **69**, 5639; L. Zhong, C. Liu, J. M. Zachara, D. W. Kennedy, J. E. Szecsody and B. Wood, *J. Environ. Qual.*, 2005, **34**, 1763.
- 66 R. Villanneau, A. Proust, F. Robert and P. Gouzerh, *Chem.–Eur. J.*, 2003, **9**, 1982.
- 67 C. Nguyen Trung, G. M. Begun and D. A. Palmer, *Inorg. Chem.*, 1992, **31**, 5280.
- 68 J. J. Berard, G. Schreckenbach, P. L. Arnold, D. Patel and J. B. Love, *Inorg. Chem.*, 2008, **47**, 11583.
- 69 M. J. Sarsfield and M. Helliwell, *J. Am. Chem. Soc.*, 2004, **126**, 1036.
- 70 S. Kannan, A. E. Vaughn, E. M. Weis, C. L. Barnes and P. B. Duval, *J. Am. Chem. Soc.*, 2006, **128**, 14024.
- 71 P. L. Arnold, D. Patel, C. Wilson and J. B. Love, *Nature*, 2008, **451**, 315.
- 72 P. J. Hay, R. L. Martin and G. Schreckenbach, *J. Phys. Chem. A*, 2000, **104**, 6259; M. C. F. Wander, S. Kerisit, K. M. Rosso and M. A. A. Schoonen, *J. Phys. Chem. A*, 2006, **110**, 9691.
- 73 F. A. Cotton, D. O. Marler and W. Schwotzer, *Inorg. Chem.*, 1984, **23**, 4211; G. Zi, L. Jia, E. L. Werkema, M. D. Walter, J. P. Gottfriedsen and R. A. Andersen, *Organometallics*, 2005, **24**, 4251.
- 74 J. P. Donahue, C. R. Goldsmith, U. Nadiminti and R. H. Holm, *J. Am. Chem. Soc.*, 1998, **120**, 12869; C. Lorber, J. P. Donahue, C. A. Goddard, E. Nordlander and R. H. Holm, *J. Am. Chem. Soc.*, 1998, **120**, 8102.
- 75 A. Yahia, P. L. Arnold, J. B. Love and L. Maron, *Chem. Commun.*, 2009, 2402–2404.